Spatial and temporal patterns of the recent warming of the Amazon forest

Juan C. Jiménez-Muñoz,[1] José A. Sobrino,[1] Cristian Mattar,[2] and Yadvinder Malhi[3]

Received 17 September 2012; revised 26 April 2013; accepted 30 April 2013; published 6 June 2013.

[1] In recent years, several studies have addressed the response of Amazonian forests to drought by analyzing anomalies in vegetation indices retrieved from satellite sensors. Attention was paid to Amazonia because of two major droughts in 2005 and 2010, which were considered amongst the most severe in a century. These drought events have been associated with increased tree mortality and a temporary shutdown of the Amazon carbon sink. The mortality has been attributed to water stress anomalies, though an additional effect might have resulted from thermal anomalies. Variations in surface temperature are believed to be closely related to drought events, but very few studies have analyzed this variable over the Amazonian region. Here we examine Moderate Resolution Imaging Spectroradiometer (MODIS) land surface temperature (LST) products from the period 2000–2012 in Amazonia. We detected anomalous warming during the dry season (July to September) in the drought years 2005 and 2010, as well as in the years 2009, 2011, and 2012 and to a lesser extent in 2008, which implies anomalous warming in 5 of the last 7 years. Recent analysis also shows warming in 2012 from June to August. Land and sea temperature records were also examined using reanalysis data from 1979 to present. Our results show good agreement between MODIS LST and reanalysis data from 2000 to present and a clear link between warming over the Amazonian region and anomalies in sea surface temperature in both the Atlantic and Pacific regions.

Citation: Jiménez-Muñoz, J. C., J. A. Sobrino, C. Mattar, and Y. Malhi (2013), Spatial and temporal patterns of the recent warming of the Amazon forest, *J. Geophys. Res. Atmos.*, *118*, 5204–5215, doi:10.1002/jgrd.50456.

1. Introduction

[2] In the context of anthropogenic global warming, there has been increased interest in examining climate trends in specific biomes, such as the tropical rainforest biome. The Amazonian region includes about one half of the world's tropical forests and is a key component of the global carbon cycle [*Cox et al*., 2000]. Moreover, relatively small changes in Amazon forest dynamics have the potential to substantially affect the concentration of atmospheric CO_2 and thus the rate of climate change itself [*Phillips et al*., 2009]. The occurrence of drought events is one major aspect of Amazonian climate change [*Malhi et al*., 2008], and its occurrence and severity is expected to increase according to several global circulation models. Two long-term drought experiments demonstrated the Amazon forest's relative resilience to drought [*Brando et al*., 2008; *da Costa et al*., 2010]. It has been also hypothesized that the tropical rainforest was able to resist under elevated temperatures and high levels of atmospheric CO_2 during the Late Paleocene-Eocene Thermal Maximum, which was one of the most abrupt global warming events of the past 65 million years [*Jaramillo et al*., 2010]. In addition, a conversion of Amazonian tropical forest to savanna due to a sustained increase in temperatures and more frequent drought events has also been predicted [*Cox et al*., 2004]. In a recent publication, some signs of a transition to a disturbance-dominated regime (versus natural variability) were observed in the southern and eastern portions of the Amazon basin [*Davidson et al*., 2012].

[3] Previous studies have linked some of the major droughts in Amazonia to the occurrence of intense El Niño events and/or strong warming in the sea surface temperature (SST) of the Tropical North Atlantic (TNA). As reviewed in *Marengo et al*. [2008], there is evidence of severe droughts in 1925–1926, 1982–1983, and 1997–1998 linked to El Niño events, in addition to evidence of droughts in 1963–1964 and 1979–1981 that were not associated with El Niño events but rather to anomalies in tropical Atlantic SST. Warming in the eastern Pacific SST (El Niño events) is particularly important for wet-season rainfall, since it suppresses convection in northern and eastern Amazonia.

Additional supporting information may be found in the online version of this article.

[1]Global Change Unit, Image Processing Laboratory, University of Valencia Science Park, Paterna, Valencia, Spain.
[2]Laboratory for Analysis of the Biosphere, Department of Environmental Sciences and Renewable Natural Resources, University of Chile, Santiago, Chile.
[3]Environmental Change Institute, School of Geography and Environment, Oxford University, Oxford, UK.

Corresponding author: J. C. Jiménez-Muñoz, Global Change Unit, Image Processing Laboratory, University of Valencia Science Park, C/Catedrático José Beltrán 2, 46980 Paterna, Valencia, Spain. (jcjm@uv.es)

2169-897X/13/10.1002/jgrd.50456

Dry-season rainfall is strongly influenced by the increase in the TNA SST (or the tropical north-south Atlantic SST gradient), which affects mostly southern and eastern Amazonia. In this case, the Intertropical Convergence Zone is shifted northward and strengthens the Hadley Cell circulation. In addition, the northeast trade winds are weakened, as is the moisture transport from the tropical Atlantic to the Amazon region [*Malhi et al*., 2008; *Marengo et al*., 2008].

[4] The study of Amazonian droughts has received increased attention due to the occurrence of two major droughts in the last decade, in 2005 and 2010. These are considered amongst the most severe in the last 100 years and are both associated with anomalies in Atlantic SST [*Marengo et al*., 2008; *Lewis et al*., 2011]. In the case of 2005, the drought led to losses of biomass resulting from increased mortality and reduced growth, which was sufficient to "switch off" the Amazonian aboveground carbon sink [*Phillips et al*., 2009]. *Phillips et al*. associated the degree of mortality with anomaly in water stress, though a more recent study [*Toomey et al*., 2011] has suggested an additional role of thermal anomalies in causing tree mortality. Previous studies also pointed out the decrease in tropical forest productivity at higher temperatures, thus reducing the capability of carbon uptake and favoring the accumulation of atmospheric CO_2. For example, *Clark et al*. [2003] found a negative correlation between tree diameter and air temperature in a tropical rain forest in Costa Rica, suggesting the potential these forests have for producing significant positive feedback toward ongoing atmospheric CO_2 accumulation, which would accelerate global warming.

[5] The impact of these droughts has been explored in several publications through remote sensing of Amazonian forest canopies, in which Moderate Resolution Imaging Spectroradiometer (MODIS) data were used in particular to analyze anomalies in Vegetation Indices (VIs) such as the Enhanced Vegetation Index (EVI) and the Normalised Difference Vegetation Index (NDVI). Results and conclusions from these studies have been controversial. Most of these controversies are reviewed in *Asner and Alencar* [2010], and they continue to be debated in some recent publications. Anomalous green-up was detected in 2005 from MODIS-derived EVI, which was interpreted as a possible increase in productivity during the drought period [*Saleska et al*., 2007]. It was later demonstrated that this result was irreproducible using an improved version of the EVI product, and it was concluded that Amazon forests did not green up during the 2005 drought [*Samanta et al*., 2010]. Positive EVI anomalies for the critical months of the 2005 drought period were also reportedly identified where forest plots had higher tree mortality, and it was concluded that positive EVI anomalies do not indicate insensitivity to droughts in Amazonian forests [*Anderson et al*., 2010]. *Brando et al*. [2010] hypothesized that drought could increase EVI by synchronizing leaf flushing via its effects on leaf bud development, whereas *Galvao et al*. [2011] demonstrated that increases in EVI during the dry season could be a consequence of solar illumination effects rather than changes on the canopy itself. In addition, *Xu et al*. [2011] reported widespread EVI negative anomalies during the dry season of the 2010 drought event, whereas *Atkinson et al*. [2011] found that NDVI and EVI anomalies for drought years (2005 and 2010) were of similar magnitude to those for nondrought years, thus concluding that it is not possible to detect the response of vegetation to drought from space using vegetation indices.

[6] In another publication, *Cho et al*. [2010] studied the relationship between Atlantic SST and Amazonian greenness using NDVI series between 1981 and 2001 extracted from Advanced Very-High Resolution Radiometer data. *Cho et al*. found a correlation between NDVI and SST in certain regions of the Amazon.

[7] Since all the previous publications used VIs retrieved from reflectance values in the visible and near-infrared spectral region, it is interesting to analyze the results obtained using data acquired in other spectral regions, for example the land surface temperature (LST) variable retrieved from Thermal Infra-Red (TIR) data. Hence, *Toomey et al*. [2011] used MODIS LST to detect thermal anomalies over the Amazonian forest during the 2005 and 2010 droughts, and they linked their results with aboveground biomass declines, also suggesting that heat stress may have played an important role (in addition to that of water stress) in the two droughts.

[8] Here we further explore the variation in LST associated with Amazonian droughts by seeking to understand the relationship between LST anomalies in Amazonia and wider climate phenomena. To do so, (1) we calculate LST anomalies over the Amazonian region using MODIS LST products during the period 2000 to 2012, (2) we extend the study period from 1979 to present using reanalysis data, and (3) we provide warming rates (slopes) using the different data sets. Since SST anomalies have played an important role in previous drought episodes, we also analyze the SST anomalies in the regions of El Niño, the Tropical North Atlantic, and the Tropical South Atlantic. The main objective of this paper is to analyze the extent, the interannual variation, and the long-term trend of thermal anomalies in Amazonia and to assess whether these thermal anomalies might be related to patterns in Pacific and Atlantic SSTs. Specifically, we ask the following questions:

[9] 1. Were the years 2005 and 2010 the only years in the last decade showing a significant thermal anomaly in Amazonia?

[10] 2. Is the updated warming rate over recent decades consistent with previously reported long-term warming rates?

[11] 3. What is the spatial pattern of temperature trends in Amazonia in recent decades?

[12] 4. Which SST region (El Niño and Tropical North and South Atlantic) shows the strongest association with the patterns of LST anomalies in Amazonia?

2. Data and Methodology

2.1. MODIS Products and Study Area

[13] We used MODIS products at 0.05° latitude/longitude Climate Modeling Grid from 2000 to 2012. Daytime and nighttime LST imagery was extracted from Terra monthly Land Surface Temperature & Emissivity product (MOD11C3) [*Wan*, 2007], and they were averaged to obtain a mean monthly temperature. The Combined Terra/Aqua yearly Land Cover product (MCD12C1) available from 2001 to 2011 was used to delimit the evergreen forest borders inside Amazonia. For this purpose, we selected Land Cover Type 1 (IGBP global vegetation classification scheme) and pixels classified as "Evergreen Broadleaf

Forest-EBF" (class 2). LST is greatly affected by changes in the land cover, so we selected the last MODIS Land Cover product available (year 2011) in order to avoid detecting significant thermal anomalies resulting from a land cover change (e.g., deforestation). The borders of the study area were delimited using a geographical vector constructed by including the surrounding South American provinces (political borders) around the Amazonian forests and then masking the EBF. A total of 189,519 pixels were included in the study area (only evergreen broadleaf forests), with an estimated ground area of about 5.81 million km^2. Figure S1 in the supporting information illustrates the delineation of the study area.

2.2. ERA-Interim Reanalysis Data

[14] The reanalysis data used included monthly means of skin temperature extracted from the ERA-Interim project developed by the European Centre for Medium-Range Weather Forecasts at $1.5° \times 1.5°$ latitude longitude global spatial resolution [*Dee et al*., 2011]. It is important to highlight that MODIS LST products were not assimilated in the reanalysis data; hence, the two data sets we compare here are completely independent of each other. ERA-Interim covers the period from 1 January 1979 onward and continues to be extended forward in near-real time. It should be noted that reanalysis data are considered more reliable from the 1980s on, as pointed out by different authors [*Bengtsson et al*., 2004a, 2004b; *Bromwich and Fogt*, 2004], mainly due to a better quality of the data and an increase in the number of measurement stations in recent decades.

[15] ERA-reanalysis calculates the skin temperature over land using a four-level self-contained soil parameterization scheme developed by *Viterbo and Beljaars* [1995] and *Viterbo et al*. [1999], in which a zero heat flux condition is set at the bottom as a boundary condition. This scheme has been tested in a stand-alone mode with the help of several long observational time series from field experiments over different sites, including the Amazonian rainforest in Brazil [*Tsuang et al*., 2008].

2.3. Anomalies and Trends

[16] We analyzed time series of monthly, seasonal, and yearly LST anomalies (in terms of both absolute and standardized anomalies, analogous to the z score in this last case). In terms of seasonal anomalies, we analyzed the four seasons January-February-March (JFM), April-May-June (AMJ), July-August-September (JAS), and October-November-December (OND). We used these four quarters in order to capture the JAS season because we observed a slight enhancement of the warming in this particular season and also because this season was considered the dry season in most of the publications dealing with anomalies in VIs (as discussed in section 1). It should be noted that the dry season in the northern quarter of Amazonia is more JFM (or December-January-February, DJF) than JAS, and even south of the equator, the peak of the dry season can vary from region to region and slightly departs from the JAS period. The reference period (climatological mean) used to compute the anomalies was 2001–2011 in the case of MODIS data and 1980–2011 in the case of ERA-Interim data.

[17] Analysis was focused on average values over the whole study area and on pixel-by-pixel values from MODIS and ERA-Interim reanalysis imagery. Since there exists markedly different seasonality among the southern, central, and northern Amazon regions, we also considered spatial averaged values over five subregions: Northwest (NW), Northeast (NE), Southwest (SW), Southeast (SE), and Central Amazon (see Figure S1.). These subregions are convenient geographical terms as opposed to references to political entities, and their selection is based on the subregions used in *Malhi and Wright* [2004]. In the case of SST analysis, values were averaged over three different regions: El-Niño 3.4 (120°W–170°W; 5°S–5°N), the Tropical North Atlantic (15°W–57.5°W; 5.5°N–23.5°N), and the Tropical South Atlantic (10°E–30°W; 0°–20°S), referred to as EN34, TNA, and TSA, respectively.

[18] A Mann-Kendall analysis [*Kendall*, 1975] was used to identify the significance of the trend in surface temperature over Amazonia, and Sen's method [*Sen*, 1968] was used to estimate the slope (warming rate). These methods are nonparametric and make no assumptions on distribution of data. Simple linear regression was also considered for visualization purposes (linear trend overplotted to the temperature records).

[19] In order to estimate the most statistically significant contribution of SST anomalies over the different regions to LST variability over Amazonia, a simple step-wise backward multiple linear regression was considered, and the coefficient of determination R^2 and F test value of significance were computed.

3. Results and Discussion

[20] This section presents and discusses the results obtained in the analysis of the warming over the Amazon forest in recent decades. First, we show the anomalies of the temperature records spatially averaged over the study area using both MODIS (2000–2012) and ERA-Interim (1979–2012) data, and then we analyze the spatial pattern of thermal anomalies during the last decade by using the high spatial resolution data (0.05°) extracted from MODIS imagery. Finally, we present the correlation between LST and SST anomalies.

3.1. Anomalies of Temperature Records

3.1.1. MODIS LSTs: 2000–2012

[21] Time series of LST anomalies extracted from MODIS data from 2000 to present are illustrated in Figure 1 for the four seasons JFM, AMJ, JAS, and OND. Time series of yearly and monthly LST anomalies are also included in Figure 1. The 2010 drought led to higher thermal anomalies than the 2005 drought did, and it provided the highest thermal anomalies of the last decade, with values around or above 0.5°C in all seasons. The warming in 2010 is especially pronounced in the JFM season, since the previous year (2009) and the following year (2011) are characterized by cooling. The AMJ season also shows warming in 2011 and 2012 (with anomalies $< +0.4$°C), whereas the JAS season shows a sustained warming from 2009 to 2012, with anomalies around or higher than +0.4°C. Warming in 2009 and 2012 is also observed in the OND season (around +0.4°C). Regarding the 2005 drought, the effect on the temperature anomalies can be observed in the AMJ season in particular,

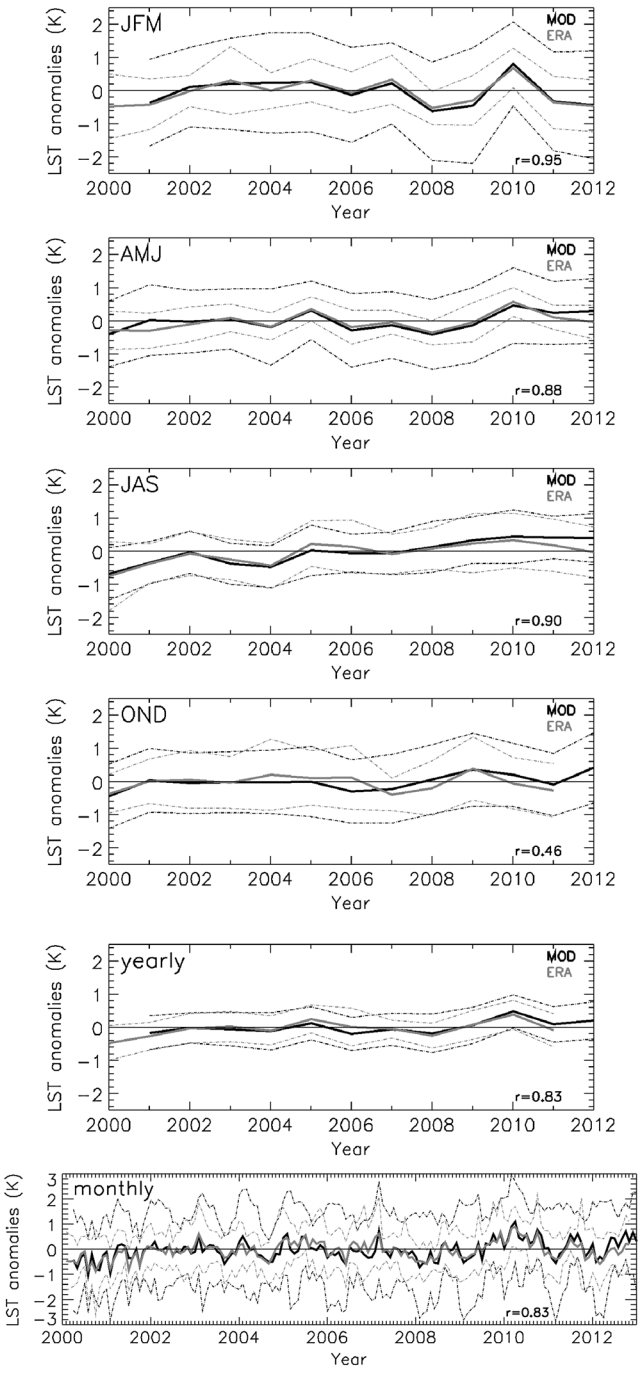

Figure 1. Seasonal (JFM, AMJ, JAS, and OND), yearly, and monthly land surface temperature (LST) anomalies (°C) extracted from MODIS LST product and ERA-Interim reanalysis data during the period 2000–2012. The linear correlation coefficient (r) between both data sets is also provided. Dashed lines refer to ±1.96 standard deviation of the mean values.

with anomalies greater than +0.2°C, and in this season, 2005 is the warmest of the first 10 years (from 2000 to 2009). In 2004, the JFM season also shows a similar level of warming to that of 2005. Note that almost a null anomaly is obtained in the JAS and OND seasons during the 2005 drought. The different warming from the two severe droughts is clearly observed in the yearly values, since in 2010 a thermal anomaly of +0.4°C is observed, while a thermal anomaly near +0.2°C is observed in 2005. This significant difference reflected in the yearly values implies that in 2010, more months provided high thermal anomalies than they did in 2005, as observed in the monthly time series, with thermal anomalies around +1°C in some months of year 2010. It is worth mentioning the anomalous cooling observed in 2000 (and to lesser extent in 2001), with anomalies below −0.5°C in all seasons and near −1°C in some months of years 2000 and 2001. Cooling is also observed in 2006 and 2008 in the JFM and AMJ seasons, in 2009 in the JFM season, and in 2004 in the AMJ season. Cooling in 2004, 2006, and 2008 is also reflected in the yearly values.

3.1.2. ERA-Interim: 1979–2012

[22] In order to check the results obtained from MODIS LST product and to analyze the long-term LST variability, we compared MODIS data to skin temperature extracted from reanalysis data in the last decade (2000–2012) (Figure 1), and the study period was extended back to 1979 in the case of reanalysis data (Figure 2). Figure 1 shows good agreement between these two independent data sets (MODIS and ERA-Interim) at monthly, seasonal, and yearly levels, indicating that reported MODIS LST anomalies are reliable and not a product artifact. Linear correlation coefficients (r) between the two data sets are higher than 0.8 and near or above 0.9 in most cases. The difference between MODIS and ERA-Interim was (0.0 ± 0.2)°C. The most significant differences between the two data sets may be the higher thermal anomalies in the JAS season for the drought of 2005 when using the ERA data and the lower thermal anomalies in the AMJ and JAS seasons in 2011 and 2012. The analysis for each individual month (not shown) shows low correlations ($r = 0.5$) between the two data sets in October and only correlations around 0.6 in November and December.

[23] On the other hand, the long-term variations (Figure 2) show that the increasing trend and sustained warming in the last decade (from 2000 to present) was not reproduced in the prior period between 1979 and 2000, even though high anomalous warming episodes also occurred in the pre-2000 period. The warming trend in the last decade is enhanced in the JAS season and to a lesser extent in the AMJ and OND seasons as well as in the yearly means and the monthly time series. The JFM season shows hardly any change in the trend between the 1979–2000 and 2000–2012 periods. The anomalous high LST observed in the pre-2000 period during the JFM season are coincident with the two major El Niño events in 1983 and 1998 (anomalies near to +1°C). Positive anomalies are also observed in other minor El Niño events: 1988 (+0.3°C), 1992 (+0.2°C), 1995 (+0.2°C), and maybe a weak El Niño event in 2010 (+0.8°C). Note that although the El Niño phenomenon is more related to the JFM (or DJF) season, the anomalous warming over Amazonia is still observed in the other seasons (note that the OND season shows warming with a lag of 1 year before the warming observed in the JFM season) and in the yearly values, especially for the huge el Niño events in 1983 and 1998.

3.1.3. Warming Rates

[24] A warming rate of 0.13 (and 95% confidence limits [0.09, 0.17]) °C/decade ($p < 0.01$) over 34 years (1979–2012) was obtained from ERA-Interim data using monthly

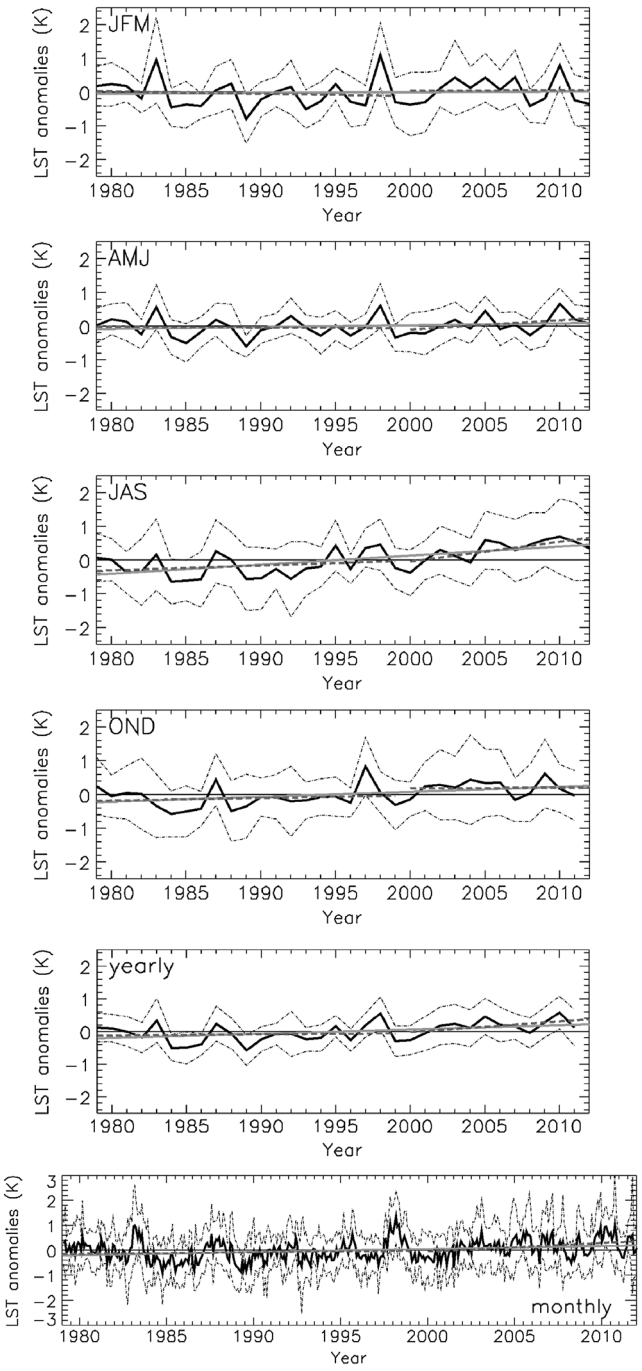

Figure 2. Seasonal (JFM, AMJ, JAS, and OND), yearly, and monthly land surface temperature (LST) anomalies (°C) extracted from ERA-Interim reanalysis data during the period 1979–2012. Linear trends for the periods 1979–2012 (continuous gray line), 1979–2000 (first dashed gray line), and 2000–2012 (second dashed gray line) are also graphed. Black dashed lines refer to ±1.96 standard deviation of the mean values.

means, whereas the warming rate increased to 0.28°C/decade ([0.15, 0.41], $p < 0.01$) when only the JAS period is considered (Table 1). This last result is in agreement with the mean annual warming rate observed from 1970 to 1998 in all tropical rainforests [*Malhi and Wright*, 2004] and also with global warming over land since 1979 [*Trenberth et al.*, 2007]. When the study period is reduced to 2000–2012, the warming rates are higher: 0.22 ([0.07, 0.38], $p < 0.01$) and 0.33°C/decade ([0.17, 0.50], $p < 0.01$) when using monthly means from ERA-Interim and MODIS data, respectively, and 0.57 ([0.11, 1.04], $p < 0.01$) and 0.89°C/decade ([0.54, 1.13], $p < 0.01$) when using respective mean values from ERA and MODIS data for the JAS period. Note that no significant trend is observed in any case during the JFM season.

[25] The previous discussion, as well as the results presented in sections 3.1.1 and 3.1.2 (Figures 1 and 2), applies to mean anomalies values obtained from spatial averages over the Amazon basin (referred to as "Global" in Table 1). Due to the high seasonal variability over the study area, basin-wide estimations are affected by high standard deviations of the mean values (as observed in Figures 1 and 2). Therefore, Table 1 also includes trends for different subregions. The most important differences between the subregions and the global values are the following:

[26] 1. ERA-Interim, 1979–2012: Significant warming is obtained over the NE and SE regions using yearly and monthly means, with slopes around +0.15°C/decade ($p < 0.01$). The warming during the JAS season is enhanced in the SE region, with a slope value almost twice the global value, +0.49°C/decade ($p < 0.01$).

[27] 2. ERA-Interim, 2000–2012: In this case, the NW region provides significant warming when using yearly and monthly means (around +0.2°C/decade, $p < 0.01$), as it does in the JAS season (+0.35°C/decade, $p < 0.01$). NW and NE regions also provide significant warming ($p < 0.05$) in the AMJ season (around +0.3°C/decade). In the JAS season, the SE region warmed at a rate of +1.22°C/decade ($p < 0.01$).

[28] 3. MODIS, 2000–2012: Slope values in the JAS season when using MODIS data are typically higher than the slope values obtained when using ERA-Interim data. The most remarkable difference when compared to the ERA results during the same period is the significant warming in the OND season for the NW (+0.48°C/decade, $p < 0.05$), SW (+0.23°C/decade, $p < 0.1$), and SE (+0.37°C/decade, $p < 0.05$) regions.

[29] A 13 year period (2000–2012) may be a very short time period for performing a climatic analysis, so values of warming rates should be taken with caution. However, the high and significant warming rate obtained in the last decade indicates a sustained warming over Amazonia in recent years. Note that the significant warming rate in the period 1979–2012 is mostly attributed to the anomalous warming in the last decade, since almost a neutral trend or slight warming is observed in the pre-2000 period (as illustrated in Figure 2). Computation of trends for the period 1979–1999 for the same cases as presented in Table 1 (results not shown) provided mostly positive slopes (warming) but with no statistical significance, except for the JAS season over the SW region (+0.21°C/decade, $p < 0.1$) and over the NW region using monthly values, with a slight cooling (−0.07°C/decade, $p < 0.1$).

3.2. Spatial Patterns of Warming

[30] In the previous section, we analyzed thermal anomalies from mean values spatially averaged over the whole study area or at most spatially averaged over certain subregions. However, since seasonal features over Amazonia vary from region to region, it is also necessary to analyze the

Table 1. Warming Rates (Slope) Over Amazonian Forests[a]

	Decadal Slope (°C decade^{-1})					
Period	Global	NW	NE	SW	SE	Central
			ERA-Interim (1979–2012)			
Yearly	0.14**	0.04	0.17***	0.08	0.18***	0.09
	(0.01, 0.27)	(−0.07, 0.14)	(0.04, 0.31)	(−0.02, 0.19)	(0.03, 0.30)	(−0.03, 0.20)
JFM	0.02	−0.04	0.03	−0.02	0.01	−0.03
	(−0.12, 0.15)	(−0.19, 0.14)	(−0.17, 0.23)	(−0.19, 0.10)	(−0.10, 0.15)	(−0.17, 0.15)
AMJ	0.06	0.01	0.10**	0.01	0.05	0.02
	(−0.05, 0.17)	(−0.09, 0.11)	(0.00, 0.21)	(−0.08, 0.11)	(−0.08, 0.21)	(−0.08, 0.12)
JAS	0.28***	0.09*	0.24***	0.21***	0.49***	0.21***
	(0.15, 0.41)	(−0.01, 0.17)	(0.10, 0.37)	(0.09, 0.33)	(0.30, 0.71)	(0.09, 0.33)
OND	0.17***	0.05	0.26***	0.08*	0.14*	0.09*
	(0.04, 0.31)	(−0.03, 0.14)	(0.06, 0.42)	(0.00, 0.17)	(−0.04, 0.28)	(−0.02, 0.19)
Monthly	0.13***	0.03*	0.15***	0.06***	0.15***	0.07***
	(0.09, 0.17)	(−0.00, 0.07)	(0.10, 0.20)	(0.02, 0.10)	(0.10, 0.21)	(0.03, 0.11)
			ERA-Interim (2000–2012)			
Yearly	0.35	0.24**	0.31	0.38	0.48***	0.36
	(−0.09, 0.79)	(0.05, 0.58)	(−0.42, 0.86)	(−0.06, 0.80)	(0.06, 0.92)	(−0.11, 0.81)
JFM	0.03	−0.03	−0.06	0.22	0.03	−0.03
	(−0.68, 1.07)	(−0.79, 0.60)	(−0.96, 1.19)	(−0.62, 1.05)	(−0.47, 0.79)	(−0.97, 1.18)
AMJ	0.25*	0.29**	0.32**	0.16	0.21	0.26
	(−0.08, 0.74)	(0.08, 0.54)	(−0.05, 0.81)	(−0.19, 0.69)	(−0.29, 0.81)	(−0.19, 0.74)
JAS	0.57***	0.35**	0.33	0.40	1.22***	0.40**
	(0.11, 1.04)	(0.10, 0.65)	(−0.27, 0.79)	(−0.53, 0.91)	(0.75, 1.82)	(−0.02, 0.81)
OND	0.03	0.20	−0.35	0.16	−0.04	0.16
	(−0.43, 0.63)	(−0.14, 0.61)	(−1.07, 0.84)	(−0.24, 0.90)	(−0.58, 0.52)	(−0.34, 0.75)
Monthly	0.22***	0.22***	0.17*	0.19	0.32***	0.22***
	(0.07, 0.38)	(0.10, 0.34)	(−0.03, 0.38)	(0.04, 0.36)	(0.15, 0.52)	(0.07, 0.38)
			MODIS (2000–2012)			
Yearly	0.27*	0.09	0.28**	0.27**	0.42***	0.17
	(−0.06, 0.68)	(−0.21, 0.71)	(−0.01, 0.69)	(0.02, 0.68)	(0.12, 0.78)	(−0.22, 0.55)
JFM	−0.12	−0.51	−0.02	−0.39	−0.24	−0.58
	(−1.08, 0.65)	(−1.49, 0.99)	(−1.14, 1.06)	(−1.12, 0.63)	(−0.66, 0.73)	(−1.77, 0.86)
AMJ	0.29	0.19	0.50**	0.40	0.38	0.24
	(−0.24, 0.85)	(−0.39, 0.94)	(0.10, 1.09)	(−0.25, 0.94)	(−0.46, 0.90)	(−0.31, 0.87)
JAS	0.89***	0.70***	0.74***	0.89***	1.15***	0.88***
	(0.54, 1.13)	(0.39, 1.06)	(0.23, 1.08)	(0.48, 1.36)	(0.79, 1.38)	(0.43, 1.25)
OND	0.32**	0.48**	0.32	0.23*	0.37**	0.11
	(−0.05, 0.68)	(0.07, 0.72)	(−0.20, 0.97)	(−0.07, 0.59)	(−0.01, 0.79)	(−0.44, 0.70)
Monthly	0.33***	0.28***	0.39***	0.37***	0.44***	0.27**
	(0.17, 0.50)	(0.09, 0.50)	(0.21, 0.59)	(0.18, 0.55)	(0.25, 0.60)	(0.05, 0.47)

[a]At basin level, "Global," and also over different subregions: NW, NE, SW, SE, and Central for different periods and using different data sets. The decadal slope refers to the increase by 10 years (decade). Values in brackets refer to minimum and maximum slope values at the 95% confidence level.
*Trend significance at the 90% confidence level.
**Trend significance at the 95% confidence level.
***Trend significance at the 99% confidence level.

spatial pattern of thermal anomalies and to assess which regions were more affected by the anomalous warming in the different periods. Figure 3 illustrates the spatial patterns of standardized anomalies using MODIS data at 0.05° spatial resolution from year 2000 to present. Only images in which a significant warming over a part of the study area was observed are shown. The first anomalous warming was observed in 2004 during the OND season (cooling was observed in years 2000 and 2001, whereas almost neutral anomalies were observed in years 2002 and 2003), followed by the warming during the drought of 2005 (note that in this case a significant warming was not observed in the JAS season). In years 2006, 2007, and 2008, significant warming was not observed, but the warming becomes significant again in year 2009 during the JAS season and is sustained until the year 2012 (except for JFM and OND seasons in 2011 and JFM season in 2012).

[31] Figure 3 shows that warmed areas are located over different regions depending on the season and the year. In 2004, only a small area of NE Amazon (around the border between Guyana and Suriname) showed significant warming. In 2005 (when the extreme drought took place), significant warming is observed over some scattered pixels in the JFM and AMJ seasons, whereas the warming is more focused in SE Amazon during the OND season. After 2 years without any significant warming (2006 and 2007) and 1 year (2008) with slight warming in the JAS and OND seasons, the warming emerges again during the JAS season in 2009 over Central and NE Amazon, and it is more widespread in the OND season, affecting almost all the subregions (except Central Amazon). In 2010, when the other extreme drought took place, significant and widespread warming is observed during the four seasons, although it vanishes in the OND season. In 2011, a small area of NE Amazon shows significant warming during the AMJ season, as is also shown in SE Amazon in the JAS season. Finally, in 2012, widespread warming is observed in the AMJ, JAS, and OND seasons. In

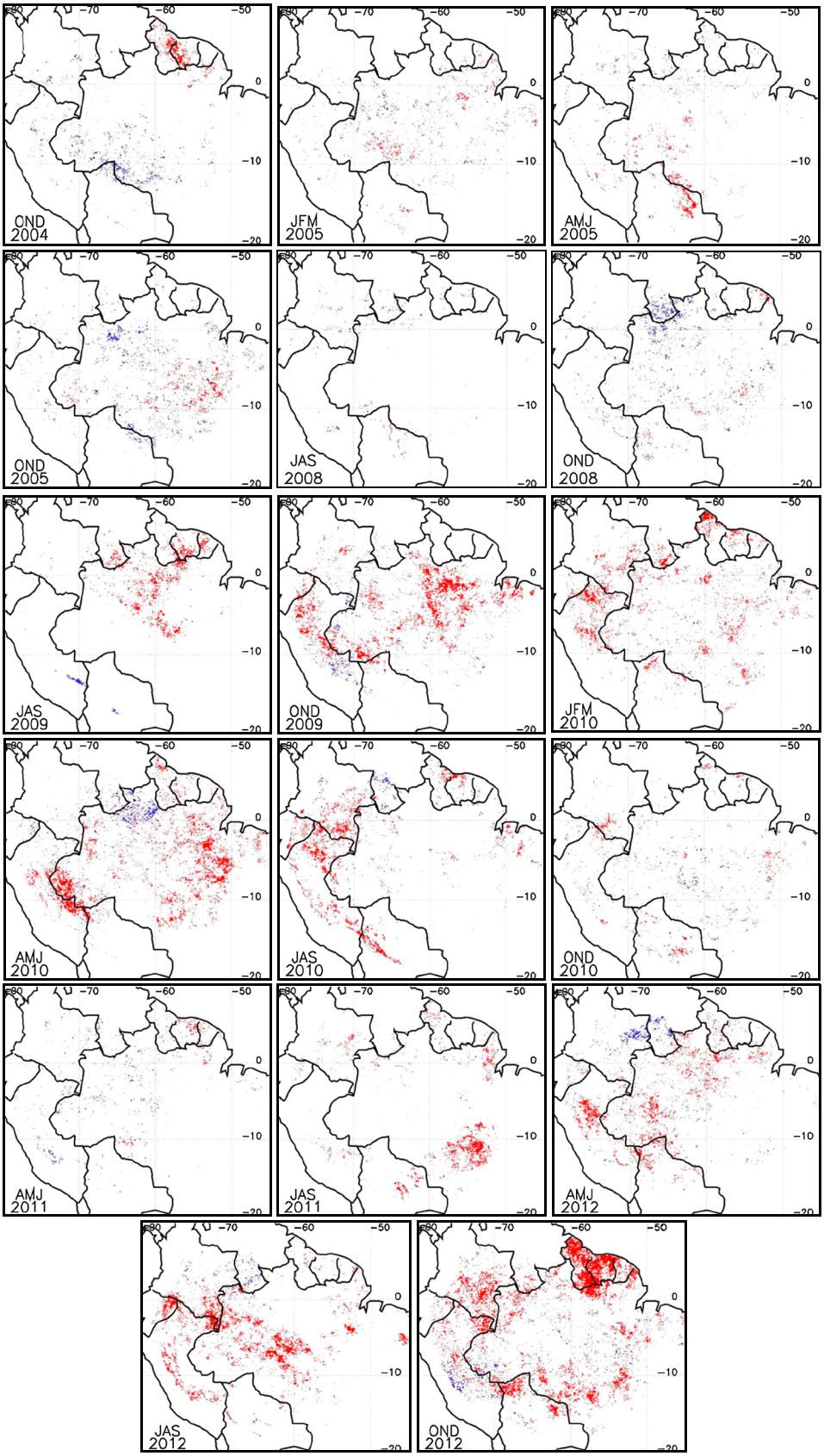

Figure 3. Spatial patterns of seasonal (JFM, AMJ, JAS, or OND) standardized anomalies in MODIS land surface temperature (LST) for the period 2000–2012. Only seasons and years where significant warming was observed have been displayed. Images are displayed in chronological order. Anomalies higher than +1.96 are colored in red, whereas anomalies lower than −1.96 are colored in blue (equivalent to $p < 0.05$).

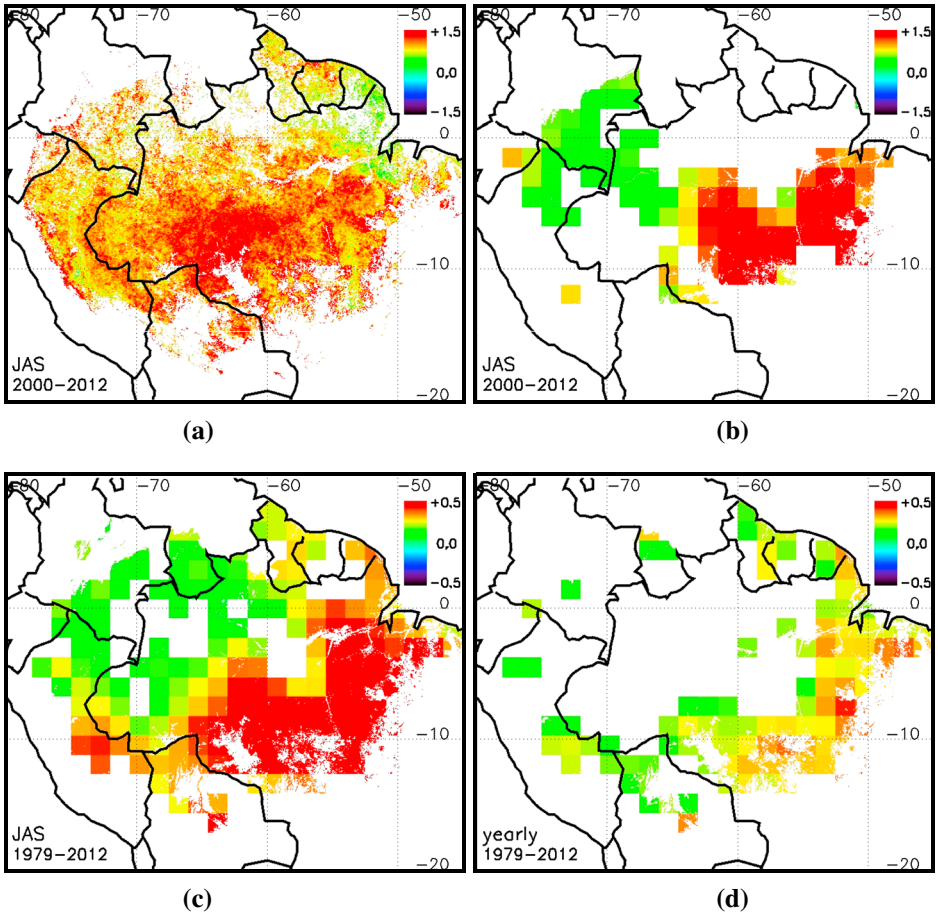

Figure 4. Spatial pattern of trends in land surface temperature (LST) (a) for the JAS season and the period 2000–2012 using MODIS data, (b) for the JAS season and the period 2000–2012 using ERA-Interim reanalysis data, (c) for the JAS season and the period 1979–2012 using ERA-Interim reanalysis data, and (d) at yearly level and the period 1979–2012 using ERA-Interim data. Only pixels with a significance at the 95% confidence level are displayed. Results refer to the slope of the trend in °C decade^{-1}.

this last case, the widespread warming over NE Amazon (Guyana, Suriname, and French Guiana) is striking.

[32] At yearly level, a weak warming is observed in 2005 and 2008 (even a cooling is observed in northern Amazonia in 2008), a stronger warming is observed in 2009 and 2011, and a strong and widespread warming is evidenced in 2010 and 2012 (Figure S2). Therefore, after the 2005 drought and probably with the exception of years 2006 and 2007, a significant warming has been sustained until the current year.

[33] We finish off the analysis of spatial patterns by computing LST trends at pixel-by-pixel basis to assess which regions notably warmed (Figure 4). The spatial distribution of the slope shows a widespread and significant ($p < 0.05$) warming over Amazonia during the JAS period both in the 2000–2012 (using MODIS data) and 1979–2012 (using ERA-Interim data) periods, with most of the affected area located in the south (~0°S–15°S), particularly in Central and SE Amazon. In this case, the warming rate for most pixels is over 1°C/decade for the period 2000–2012 and over 0.5°C/decade for the period 1979–2012. On the contrary, the NW Amazon shows a significant warming trend but substantially lower slope values than SE Amazon. Note also that the spatial pattern of LST trends obtained from MODIS and ERA data sets (Figures 4a and 4b) are consistent, except for a region in NE Amazon (Guyana, Suriname, and French Guiana) where MODIS-derived trends are significant and ERA-derived trends do not show any significant trend, at least at $p < 0.05$. Figure S3 (auxiliary material) shows results obtained for other seasons (JFM, AMJ, and OND). There is hardly any observable trend over the whole study area in the JFM season or even in the AMJ season (although in this case significant values are obtained for some pixels in NE Amazon). Trends obtained from ERA-Interim data for the OND season show significant warming just at the borders of the study area, which may be explained by the lower spatial resolution of this data set (border effect).

3.3. The Role of SST Anomalies

[34] As discussed in section 3.1.2, the long-term variability of the LST over Amazonia (Figure 2) shows anomalous high warming related to warm SST anomalies in the eastern Pacific (El Niño). However, from 2000 to 2011, powerful El Niño events were not reported, but anomalous warming was observed over Amazonia over this period (especially in the final years, 2009–2012; Figure 3). In this section, we analyze whether SST anomalies in the Atlantic also played a role in the warming over Amazonia. Figure 5 shows the long-term LST variability in Amazonia (global averages)

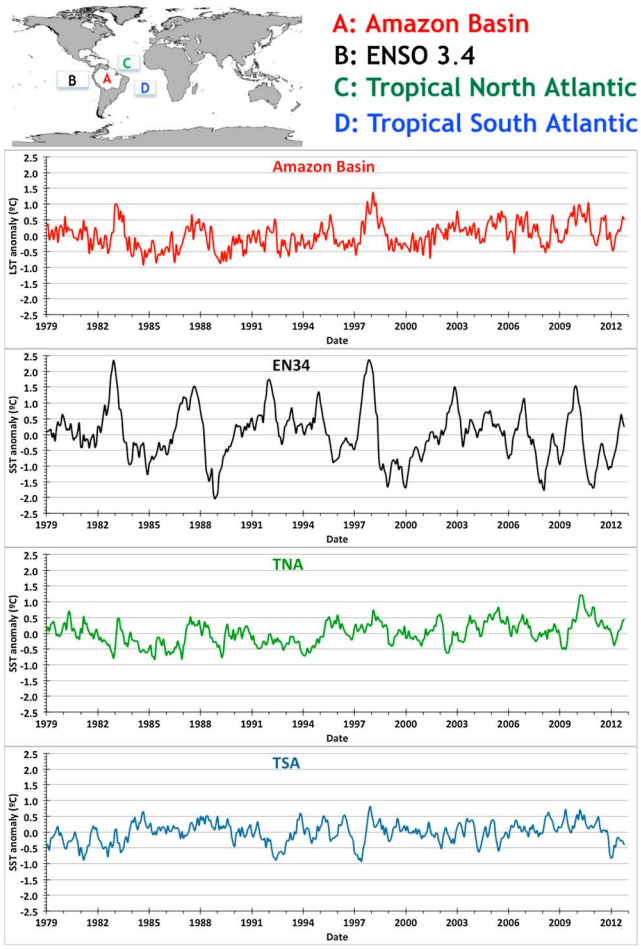

Figure 5. Time series of monthly LST anomalies over the Amazonian region and monthly SST anomalies over the El Niño 3.4 region and the tropical North and South Atlantic regions. Results obtained from ERA-Interim reanalysis data over the period 1979–2012.

compared to SST anomalies in EN34, TNA, and TSA regions using ERA-Interim data. Analysis by simple linear regression (Table 2) shows that monthly SST-EN34 anomalies explained 19% ($p < 0.01$) of the monthly LST variability over Amazonia, and SST-TNA anomalies explained 31% ($p < 0.01$) of the variability. Both SST EN34 and TNA anomalies explained 48% ($p < 0.01$) of the LST variability, whereas almost no contribution of SST-TSA anomalies was found. The different contributions of SST EN34 and TNA are clearly observed when JFM and JAS seasons are compared: when we use seasonal values for the JFM period, SST-EN34 and SST-TNA anomalies explained respectively 61% ($p < 0.01$) and 36% ($p < 0.01$) of the LST variability (and more than 77% when both EN34 and TNA regions are considered), whereas when we use seasonal values for the JAS period, SST-TNA anomalies explained 40% ($p < 0.01$) of the LST variability, and the SST-EN34 anomalies did not contribute to this variability. SST-EN34 anomalies also show a significant contribution for the AMJ (22%, $p < 0.01$) and OND (31%, $p < 0.01$) seasons, whereas SST-TNA anomalies show a significant contribution in all four seasons, especially in the OND season with a R^2 of 50% ($p < 0.01$). Note that SST-TSA anomalies did not contribute to the LST variability over Amazonia. When we focus on the different subregions, the SST-EN34 anomalies show the highest contribution to LST variability over NE Amazon at monthly level and for the OND season as well, whereas in the JFM or AMJ seasons the rest of subregions show similar correlations. The high contribution of SST-TNA to LST variability over NW Amazon in the OND season (57%, $p < 0.01$) is also observable, whereas in the JAS season the highest correlation was obtained over SE and Central Amazon (37%, p 0.01). Therefore, both the EN34 and TNA regions influence the climate over the Amazonia, though each region contributes differently in different seasons. Although the TSA region did not show any contribution to the LST variability (except for the OND season over SW and Central Amazon, with $R^2 < 15\%$), this region might also play a role through the gradient between TNA and TSA [*Harris et al.*, 2008]. This option, however was not explored in this paper. The spatial pattern of the correlation (Figure 6) corroborates the results presented in Table 2, with a widespread effect of SST anomalies in the EN34 region on the LST over Amazo-

Table 2. R^2 From Simple Linear Regression of LST Anomalies in Amazonian Forests[a]

	Region	EN34	TNA	TSA	EN34 + TNA
Yearly	Global	0.089*	0.608***	0.000	0.739***
	NW	0.057	0.501***	0.010	0.589***
	NE	0.192**	0.416***	0.015	0.658***
	SW	0.115*	0.438***	0.002	0.592***
	SE	0.030	0.657***	0.000	0.714***
	Central	0.095*	0.566***	0.002	0.703***
JFM	Global	0.614***	0.361***	0.033	0.774***
	NW	0.381***	0.330***	0.006	0.557***
	NE	0.632***	0.284***	0.025	0.738***
	SW	0.640***	0.230***	0.049	0.713***
	SE	0.533***	0.396***	0.017	0.731***
	Central	0.614***	0.296***	0.045	0.730***
AMJ	Global	0.221***	0.461***	0.030	0.612***
	NW	0.230***	0.481***	0.024	0.638***
	NE	0.158**	0.391***	0.003	0.494***
	SW	0.328***	0.322***	0.051	0.578***
	SE	0.183**	0.455***	0.058	0.575***
	Central	0.239***	0.404***	0.039	0.574***
JAS	Global	0.002	0.399***	0.001	0.420***
	NW	0.007	0.331***	0.001	0.363***
	NE	0.091*	0.243***	0.028	0.392***
	SW	0.001	0.293***	0.007	0.308**
	SE	0.014	0.367***	0.002	0.368***
	Central	0.014	0.368***	0.012	0.415***
OND	Global	0.310***	0.503***	0.062	0.848***
	NW	0.098*	0.572***	0.053	0.691***
	NE	0.319***	0.357***	0.001	0.706***
	SW	0.221***	0.357***	0.139**	0.603***
	SE	0.296***	0.346***	0.066	0.670***
	Central	0.282***	0.358***	0.143**	0.669***
Monthly	Global	0.193***	0.308***	0.001	0.476***
	NW	0.110***	0.258***	0.000	0.351***
	NE	0.260***	0.228***	0.000	0.463***
	SW	0.163***	0.187***	0.004	0.331***
	SE	0.093***	0.251***	0.000	0.328***
	Central	0.204***	0.223***	0.007	0.405***

[a]At basin level, "Global," and also over different subregions: NW, NE, SW, SE, and Central versus SST anomalies in the El Niño 3.4 (EN34), Tropical North Atlantic (TNA), and Tropical South Atlantic (TSA) regions. Results were obtained using ERA-Interim data for the period 1979–2012.
*F test value of significance at the 90% confidence level.
**F test value of significance at the 95% confidence level.
***F test value of significance at the 99% confidence level.

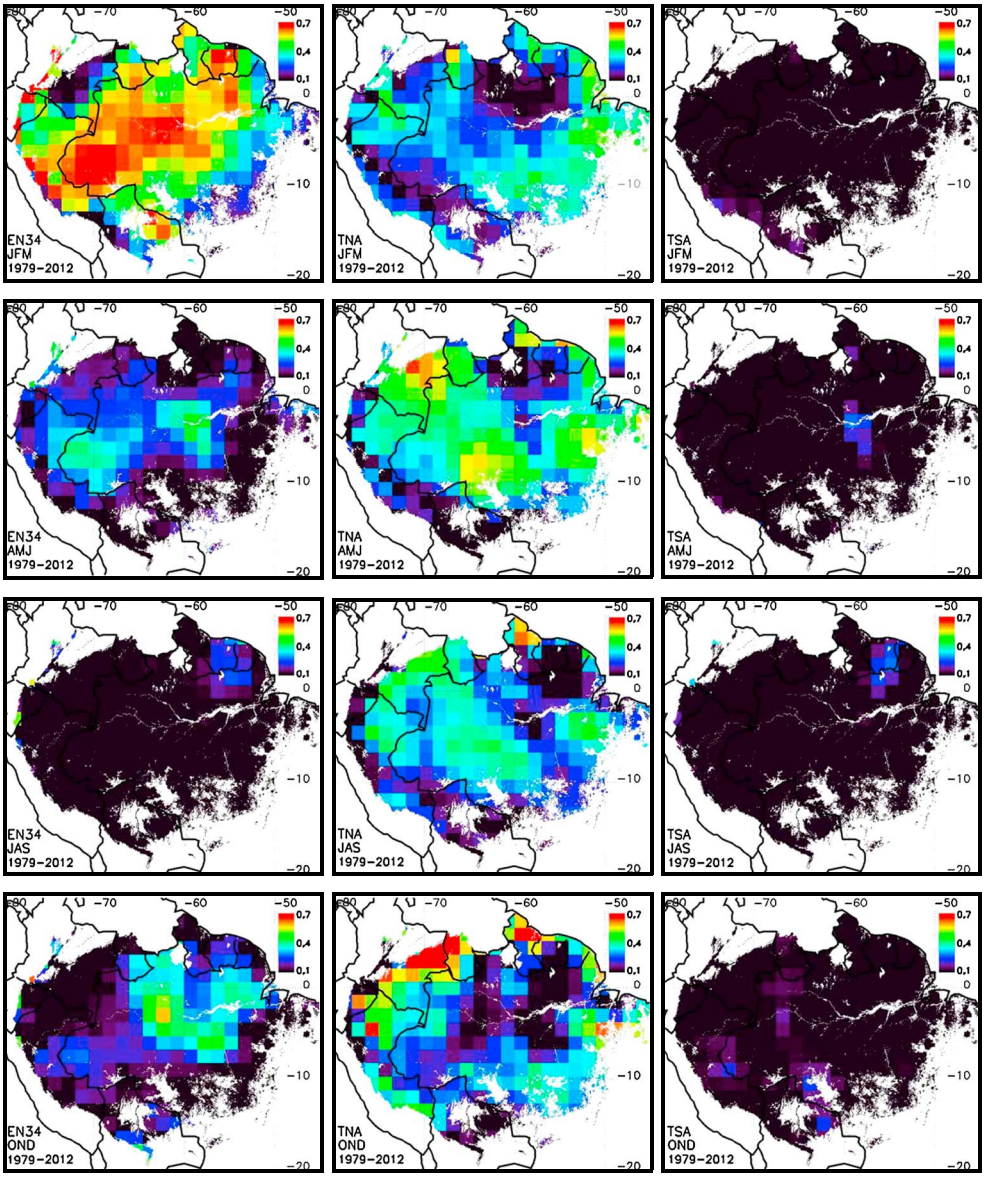

Figure 6. Spatial patterns of R^2 from simple linear regression of LST anomalies in Amazonian forests versus SST anomalies in El Niño 3.4 (EN34), Tropical North Atlantic (TNA), and Tropical South Atlantic (TSA) regions. Results obtained from ERA-Interim reanalysis data over the period 1979–2012.

nia in the DJF season, in addition to a widespread effect of SST-TNA anomalies on the LST in the AMJ, JAS, and OND seasons. It can also be observed that the correlation increases in the case of EN34 and TNA with a 2 month lag (Figure S4). The link between warm LST anomalies over Amazonia and warm SST anomalies in the different sea regions can be observed by analyzing the spatial patterns of SST anomalies for the different warming episodes (Figure S5). This analysis shows that warming over Amazonia can be induced by different anomalous situations related to different warmed sea regions (and different seasons as well): (i) warm SST anomalies in the EN34 region (e.g., El Niño events in 1983, 1987, 1992, 1995, and 1998), (ii) warm SST anomalies in the TNA region or strong gradient between SST-TNA and SST-TSA (e.g., JAS season in 2010 and 2011), and (iii) warm SST anomalies in both the Pacific and Atlantic regions (e.g., JFM-2010 or JAS-2012).

[35] The results discussed in this section describe how the warming over Amazonia is related to warming in different combinations of sea regions. Since the 2010 drought led to the highest thermal anomalies over Amazonia, it seems that the occurrence of warm anomalies in the three regions (EN34, TNA, TSA) during the DJF season, in combination with the occurrence of warm anomalies in both the TNA and TSA regions during the JAS season, is an especially favorable condition for causing intense and widespread warming over the Amazonian tropical forests.

4. Conclusions

[36] Significant and sustained warming was evidenced over Amazonia during the last decade (2000–2012), especially in the droughts of 2005 and 2010, though also in the post-drought years 2011 and 2012. Isolated warming

episodes were also found in the pre-2000 period (1979–1999), but trends in LST during this period were almost neutral or slightly positive. The recent warming episodes over Amazonia have been found to be related to SST anomalies in the tropical Atlantic during the JAS period and SST anomalies in the central/east Pacific during the JFM season. However, it was also found that Atlantic and Pacific SST anomalies combine in different ways and seasons to induce warming over Amazonia, and warm SST anomalies in the tropical Atlantic were also found during the JFM season prior to the observed warming over Amazonia in the JAS period. Both SST-EN34 and SST-TNA anomalies explained more than 70%, 60%, and 40% ($p < 0.01$) of the LST variability over Amazonia in the JFM, AMJ, and JAS seasons, respectively, and up to 85% in the OND season. Since SST anomalies lead to atmospheric perturbations affecting the Amazon Basin climate [*Harris et al*., 2008], thermal anomalies over Amazonia are part of a wider atmosphere-ocean response. According to *Toomey et al*. [2011], water and heat stress led to biomass losses in the 2005 and 2010 droughts. Therefore, the atmospheric responses to regional patterns of SST anomalies lead to anomalous warming over Amazonia, which in turn leads to aboveground biomass decline. In addition, this biomass decline may cause a rise in surface temperature and enhance the warming. If SST conditions associated to the Amazonian warming become much more common in the future [*Cox et al*., 2008], a feedback mechanism could be "switched on," and the forest resilience to warming events could be weakened, since increased temperature can be more important than precipitation reduction in causing the losses of biomass [*Galbraith et al*., 2010].

[37] On the other hand, the spatial distribution of trends (with a strong warming in the SE Amazonia) is consistent with the climatic gradient across the Amazon basin from continuously wet conditions in the northwest (with low warming rates) to long and pronounced dry seasons in the southeast [*Davidson et al*., 2012]. This result also suggests an interaction between local land use change and broader warming, since deforestation practices are mostly performed over SE Amazon.

[38] The fact that the warming in 2005 is significantly weaker than the warming in 2010, jointly with the fact that years 2006 and 2007 did not show warming but post-drought years 2011 and 2012 did show a widespread and significant warming, suggests a loss of resilience of the Amazon forest to drought, although analysis of LST anomalies in the years to come is required to extract strong conclusions.

[39] **Acknowledgments.** We acknowledge funding from European Union (CEOP-AEGIS, project FP7-ENV-2007-1 Proposal No. 212921) and Ministerio de Economía y Competitividad (EODIX, project AYA2008-0595-C04-01; CEOS-Spain, project AYA2011-29334-C02-01). We thank the MODIS and ERA-Interim projects for providing the data used in this paper and the anonymous reviewers for constructive comments on the manuscript.

References

Anderson, L. O., Y. Malhi, L. E. O. C. Aragao, R. Ladle, E. Arai, N. Barbier, and O. Phillips (2010), Remote sensing detection of droughts in Amazonian forest canopies, *New Phytol.*, *187*, 733–750.

Asner, G. P., and A. Alencar (2010), Drought impacts on the Amazon forest: The remote sensing perspective, *New Phytol.*, *187*, 569–578.

Atkinson, P. M., J. Dash, and C. Jeganathan (2011), Amazon vegetation greenness as measured by satellite sensors over the last decade, *Geophys. Res. Lett.*, *38*, L19105, doi:10.1029/2011GL049118.

Bengtsson, L., S. Hagemann, and K. I. Hodges (2004a), Can climate trends be calculated from reanalysis data?, *J. Geophys. Res.*, *109*, D11111, doi:10.1029/2004JD004536.

Bengtsson, L., K. I. Hodges, and S. Hagemann (2004b), Sensitivity of the ERA40 reanalysis to the observing system: Determination of the global atmospheric circulation from reduced observation, *Tellus A*, *56*(5), 456–471.

Brando, P. M., D. C. Nepstad, E. A. Davidson, S. E. Trumbore, D. Ray, and P. Camargo (2008), Drought effects on litterfall, wood production and belowground carbon cycling in an Amazon forest: Results of a throughfall reduction experiment, *Phil. Trans. R. Soc. B*, *363*, 1839–1848.

Brando, P. M., S. J. Goetz, A. Baccini, D. C. Nepstad, P. S. A. Beck, and M. C. Christman (2010), Seasonal and interannual variability of climate and vegetation indices across the Amazon, *Proc. Natl. Acad. Sci. U.S.A.*, *107*(33), 14,685–14,690, doi:10.1073/pnas.0908741107.

Bromwich, D., and R. Fogt (2004), Strong trends in the skill of the ERA-40 and NCEP NCAR Reanalysis in the high and midlatitudes of the Southern Hemisphere, 1958–2001, *J. Climate*, *17*, 4603–4619.

Clark, D. A., S. C. Piper, C. D. Keeling, and D. B. Clark (2003), Tropical rain forest tree growth and atmospheric carbon dynamics linked to interannual temperature variation during 1984-2000, *Proc. Natl. Acad. Sci. U.S.A*, *100*(10), 5852–5857, doi:10.1073/pnas.0935903100.

Cho, J., P. J.-F. Yeh, Y.-W. Lee, H. Kim, T. Oki, S. Kanae, W. Kim, and K. Otsuki (2010), A study on the relationship between Atlantic sea surface temperature and Amazonian greenness, *Ecol. Inform.*, *5*, 367–378.

Cox, P. M., R. A. Betts, C. D. Jones, S. A. Spall, and I. J. Totterdell (2000), Acceleration of global warming due to carbon-cycle feedbacks in a coupled climate model, *Nature*, *393*, 249–252.

Cox, P. M., R. A. Betts, M. Collins, C. Harris, C. Huntingford, and C. D. Jones (2004), Amazonian forest dieback under climate-carbon cycle projections for the 21st century, *Theor. Appl. Climatol.*, *78*, 137–156.

Cox, P. M., P. P. Harris, C. Huntingford, R. A. Betts, M. Collins, C. D. Jones, T. E. Jupp, J. A. Marengo, and C. A. Nobre (2008), Increasing risk of Amazonian drought due to decreasing aerosol pollution, *Nature*, *453*, 212–216.

da Costa, A. C. L., *et al*. (2010), Effect of 7 yr experimental drought on vegetation dynamics and biomass storage of an eastern Amazonian rainforest, *New Phytol.*, *187*, 579–591.

Davidson, E. A., et al. (2012), The Amazon basin in transition, *Nature*, *481*, 321–328.

Dee, D. P., *et al*. (2011), The ERA interim reanalysis: Configuration and performance of the data assimilation system, *Q. J. R. Meteorol. Soc.*, *137*, 553–597.

Galbraith, D., P. E. Levy, S. Sitch, C. Huntingford, P. Cox, M. Williams, and P. Meir (2010), Multiple mechanisms of Amazonian forest biomass losses in three dynamic global vegetation models under climate change, *New Phytol.*, *187*, 647–665, doi:10.1111/j.1469-8137.2010.03350.x.

Galvao, L. S., J. R. dos Santos, D. A. Roberts, F. Marcelo Breunig, M. Toomey, and Y. M. de Moura (2011), On intra-annual EVI variability in dry season of tropical forest: A case study with MODIS and hyperspectral data, *Remote Sens. Environ.*, *115*, 2350–2359.

Harris, P. P., C. Huntingford, and P. M. Cox (2008), Amazon Basin climate under global warming: The role of the sea surface temperature, *Phil. Trans. R. Soc. B*, *363*, 1753–1759.

Jaramillo, C., et al. (2010), Effects of rapid global warming at the Paleocene-Eocene boundary on neotropical vegetation, *Science*, *330*, 957–961.

Kendall, M. G. (1975), *Rank Correlation Methods*, 4th ed., 196 p., Charles Griffin, London.

Lewis, S. L., P. M. Brando, O. L. Phillips, G. M. F. vand der Heijden, and D. Nepstad (2011), The 2010 Amazon drought, *Science*, 331, 554.

Malhi, Y., and J. Wright (2004), Spatial patterns and recent trends in the climate of tropical rainforest regions, *Phil. Trans. R. Soc. Lond. B*, *359*, 311–329.

Malhi, Y., J. Timmons Roberts, R. A. Betts, T. J. Killeen, W. Li, and C. A. Nobre (2008), Climate change, deforestation, and the fate of Amazon, *Science*, *319*, 169–172.

Marengo, J. A., C. A. Nobre, J. Tomasella, M. D. Oyama, G. S. de Oliveira, R. de Oliveira, H. Camargo, L. M. Alves, and I. Foster Brown (2008). The drought of Amazonia in 2005, *J. Clim.*, *21*(3), 495–516.

Phillips, O. L., et al. (2009), Drought sensitivity of the Amazon rainforest, *Science*, *323*, 1344–1347.

Saleska, S. R., K. Didan, A. R. Huete, and H. R. da Rocha (2007), Amazon forests green-up during 2005 drought, *Science*, *318*, 612.

Samanta, A., S. Ganguly, H. Hashimoto, S. Devadiga, E. Vermote, Y. Knyazikhin, R. R. Nemani, and R. B. Myneni (2010), Amazon forest did not green-up during the 2005 drought, *Geophys. Res. Lett.*, *37*, L05401, doi:10.1029/2009GL042154.

Sen, P. K. (1968). Estimates of the regression coefficient based on Kendall's tau, *J. Am. Stat. Assoc.*, *63*, 1379–1389.

Toomey, M., D. A. Roberts, C. Still, M. L. Goulden, and J. P. McFadden (2011), Remotely sensed heat anomalies linked with Amazonian forest biomass declines, *Geophys. Res. Lett.*, *38*, L19704, doi:10.1029/2011GL049041.

Trenberth, K. E., et al. (2007), Observations: Surface and atmospheric climate change, in *Climate Change 2007: The Physical Science Basis*, edited by S. Solomon, et al., pp. 236–336, Cambridge University Press, Cambridge, United Kingdom and New York, NY, USA.

Tsuang, B.-J., M.-D. Chou, Y. Zhang, A. Roesch, and K. Yang (2008), Evaluations of land–ocean skin temperatures of the ISCCP satellite retrievals and the NCEP and ERA Reanalyses, *Bull. Am. Meteorol. Soc.*, doi:10.1175/2007JCLI1502.1.

Viterbo, P., and A. C. M. Beljaars (1995), An improved land surface parameterization scheme in the ECMWF model and its validation, *J. Climate*, *8*, 2716–2748.

Viterbo, P., A. C. M. Beljaars, J. F. Mahfouf, and J. Teixeira (1999), The representation of soil moisture freezing and its impact on the stable boundary layer, *Quart. J. Roy. Meteor. Soc.*, *125*, 2401–2426.

Wan, Z. (2007), *Collection-5 MODIS Land Surface Temperature Products Users' Guide*, 30 p., ICESS, University of California, Santa Barbara.

Xu, L., A. Samanta, M. H. Costa, S. Ganguly, R. R. Nemani, and R. B. Myneni (2011), Widespread decline in greenness of Amazonian vegetation due to the 2010 drought, *Geophys. Res. Lett.*, *38*, L07402, doi:10.1029/2011GL046824.